VIIRS/SUOMI-NPP WATER VAPOR PRODUCTS ALGORITHM THEORETICAL BASIS DOCUMENT

Version 1.0

E. EVA BORBAS, ZHENGLONG LI, W. PAUL MENZEL,
LAURA DOBOR, MATYAS RADA and BRUCE FLYNN

University of Wisconsin-Madison 1225 W. Dayton St.
Madison, WI 53706

July 19, 2019

[1]Cooperative Institute for Meteorological Satellite Studies (Eva.Borbas@ssec.wisc.edu)

Revisions

Change record			
Version	**Date**	**Author/changed by**	**Remarks**
0.5	May 1, 2018	E.E. Borbas (UW/SSEC)	Initial draft
0.6	Apr 14, 2019	E. E Borbas	Update
0.7	Jun 28, 2019	W. P. Menzel	Review
0.7	July 19, 2019	E.E. Borbas	Deliver to NASA for review
0.8	Aug 5, 2019	B. Ramachandran	Review
0.9	Sept 25, 2019	E.E. Borbas	2nd deliver to NASA for review
0.91	Nov 22, 2019	B. Ramachandran	2nd review
1.0	Nov 25, 2019	E.E. Borbas	Final version

Table of Contents

1. Introduction

The purpose of this document is to present an algorithm for retrieving atmospheric moisture from multi-wavelength thermal radiation measurements in clear skies. While the VIIRS is not a sounding instrument, it does have some of the spectral bands useful for integrated total column water vapor. The VIIRS algorithms were adapted from the MODIS algorithm, with adjustments to accommodate the absence of some sounding spectral bands and to realize the advantage of greatly increased spatial resolution (0.750 km) with good radiometric signal to noise (better than 0.35 K for typical scene temperatures in all spectral bands).

We provide total column water vapor properties from merged VIIRS infrared measurements and CrIS plus ATMS water vapor soundings to continue the depiction of global moisture at high spatial resolution started with MODIS. While MODIS has two channels within the 6.5-μm H_2O band and four channels within the 15-μm CO_2 band, VIIRS has no infrared (IR) absorption channels. However, the VIIRS IR windows at 8.6, 10.8 and 12-μm give some indication of low level moisture (which constitutes much of the total column amount) and we complement this with CrIS+ATMS (or later referred also as CrIS/ATMS) column moisture determinations. This VIIRS+CrIS/AMTS algorithm follows the approach used for MODIS. A clear sky regression relationship has been established between total precipitable water vapor (TPW) and VIIRS IR window brightness temperatures (BTs) and the CrIS/ATMS water vapor soundings calculated from a global training radiosonde-based profile data set. A high spatial resolution surface emissivity database is used to help differentiate surface emission and atmospheric moisture absorption. CrIS/ATMS is added in clear and partly cloudy regions to enhance the TPW depiction and to extend the spatial coverage.

During the combined VIIRS + CrIS/ATMS algorithm development period, there have been two CrIS or CrIS/ATMS TPW products available: the UW/SSEC Dual Regression (DR) single FOV CrIS retrievals (Smith et al., 2012) and the NUCAPS (NOAA Unique CrIS ATMS Processing System, Gambacorta, 2013) retrievals. While the DR has a better spatial resolution data (single CrIS FOV at 14km), that algorithm provides TPW only over clear or very low cloud scenes. On the other hand, the NUCAPS water vapor product is available over clear and most cloudy scenes but with a much lower spatial resolution (single ATMS FOV at 45km). The NUCAPS TPW has been selected for use in the VIIRS+CrIS/ATMS TPW algorithm because of its much better spatial coverage.

Figure 1 shows a normalized histogram of MYD07 vs VIIRS (5km) and NUCAPS TPW for the global day in Oct 15, 2014 over water scenes separated by morning and afternoon. Comparing the VIIRS-only and NUCAPS TPW products to the MYD07 TPW distribution, VIIRS-only product and NUCAPS products appear to be complementary. For example, the VIIRS-only overestimates TPW for both dry scenes (smaller than 15 mm) and wet scenes (larger than 55 mm) while NUCAPS underestimates them. Overall, the VIIRS plus NUCAPS (CrIS/ATMS) algorithm shows promise for continuing the moisture records established by MODIS.

In this ATBD, we offer some background to the retrieval problem, review the VIIRS instrument and NUCAPS product characteristics, describe the theoretical basis of the retrieval algorithm, discuss the practical aspects of the algorithm implementation, present the gridding and aggregation of the Level-3 products, and provide some validation of the Level-2 and Level-3 water vapor (WATVP) products.

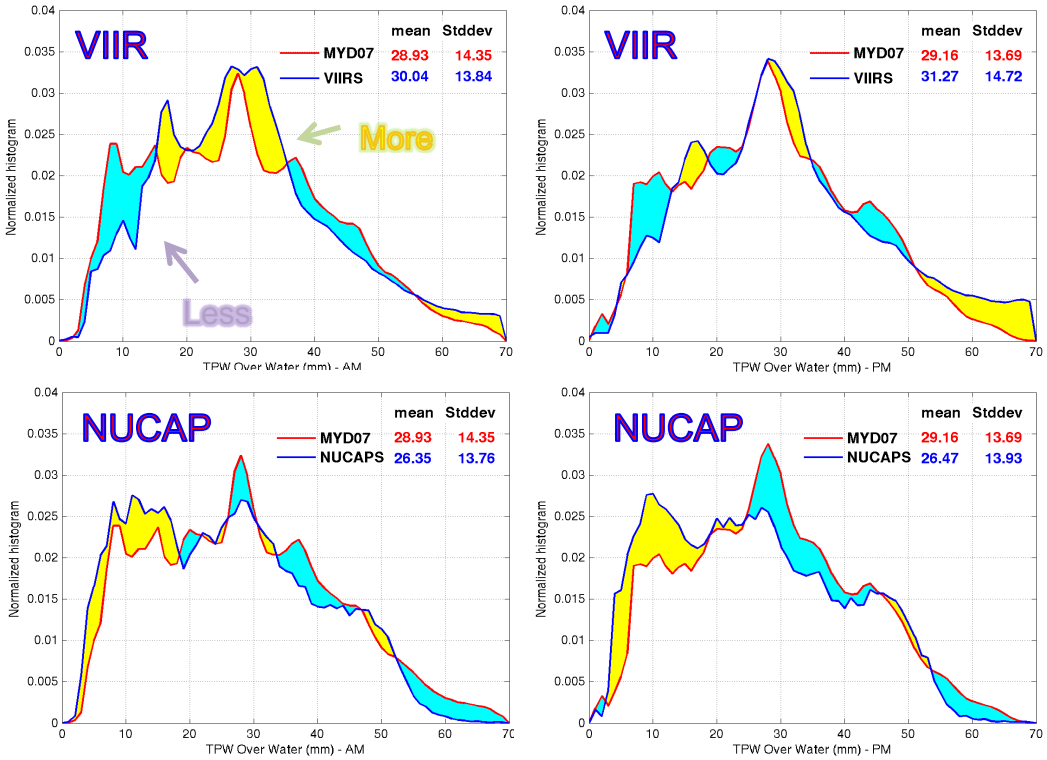

Figure 1: Normalized histogram of MYD07 vs VIIRS (5km) (top panels) and NUCAPS TPW (bottom panels) on Oct 15, 2014 over water separated by the morning (left panels) and afternoon granules (right panels) .

1. Instrument Characteristics

The following sections describe the current state of the S-NPP VIIRS, CrIS and ATMS instruments.

1.1. VIIRS

The VIIRS sensor is a 22-band scanning radiometer that is currently flying on the NASA S-NPP platform. 16 channels are at 750-m resolution (medium resolution, or M bands) and 5 channels at 375 m resolution (imaging bands, or I bands), and in addition there is a day/night band at 750-m resolution. For this investigation, the focus will be on using the infrared M bands. VIIRS has 2 bands in short-wave IR region and 3 bands in long-wave IR region. To avoid the impact from solar contamination, for this study, only the 3 long-wave bands (8.55, 10.7, and 12 μm) will be used for the TPW retrieval.

1.2. CrIS plus ATMS

The CrIS, a Fourier transform spectrometer, has 1305 spectral channels over 3 wavelength ranges: longwave IR (9.14 - 15.38 μm); midwave IR (5.71 - 8.26 μm); and shortwave IR (3.92 - 4.64 μm). CrIS scans a 2200 km swath width (+/- 50 degrees of scanning angle), with 30 Earth-scene views, also known as Field Of Regard (FOR). Each FOR consists of 9 fields of view, arrayed as 3x3 array of 14 km diameter spots (nadir spatial resolution). A primary purpose for CrIS is the determination of high-resolution, three-dimensional temperature, pressure, and moisture profiles. The Advanced Technology Microwave Sounder (ATMS), a cross-track

microwave scanner with 22 channels, provides sounding observations required to retrieve profiles of atmospheric temperature and moisture in clear as well as non-precipitating cloudy conditions for civilian operational weather forecasting as well as continued measurements for climate monitoring purposes. The NUCAPS (Gambacorta, 2013) combines the CrIS and ATMS to provide 45 km resolution soundings of temperature, moisture, and ozone. The NUCAPS consist of two types of environmental data record (EDR) products: the standard atmospheric sounding products and the cloud-cleared radiance products. The sounding retrieval is a two-stage process. The first stage, the microwave (MW)-only retrieval, generates the first guess temperature/moisture profile, along with cloud amount, height, and surface skin temperature. A simultaneous physical retrieval is then performed with both IR and MW radiances to generate an improved sounding EDR product. The NUCAPS sounding EDR products are available in both clear and cloudy regions; they have been validated and errors have been characterized (Sun et al., 2017).

2. Algorithm Description

In this section we describe the theoretical basis and practical implementation of the atmospheric profile retrieval algorithm.

2.1. *Theoretical Background*

The VIIRS algorithm retrieves total column precipitable water vapor. This statistical regression retrieval algorithm is performed using clear sky radiances (brightness temperatures) measured by VIIRS over land and ocean for both day and night. The retrieval methods are based on the work of Borbas et al. (2011), Seemann et al. (2003 and 2008), Li (2000), Smith and Woolf (1988), and Hayden (1988).

The operational VIIRS water vapor retrieval algorithm consists of the regression coefficient calculation, which includes forward model calculation, and the regression retrieval. The radiative transfer calculation of the VIIRS emissive spectral band radiances is performed using a transmittance model called the Joint Center for Satellite Data Assimilation (JCSDA) Community Radiative Transfer Model (CRTM, Han et al., 2005). The calculations take into account the satellite zenith angle, absorption by well-mixed gases (including nitrogen, oxygen, and carbon dioxide), water vapor (including the water vapor continuum), and ozone.

2.2. Statistical Regression Retrieval

A computationally efficient method for determining temperature and moisture profiles from satellite sounding measurements uses previously determined statistical relationships between observed (or modeled) radiances and the corresponding atmospheric profiles. This method is often used to generate a first-guess for a physical retrieval algorithm, as is done in the International TOVS* Processing Package (ITPP, Smith et al., 1993). The statistical regression algorithm for atmospheric temperature is described in detail in Smith et. al. (1970), and can be summarized as follows (the algorithm for moisture profiles is formulated similarly). In cloud-free skies, the radiation received at the top of the atmosphere at frequency ν is the sum of the radiance contributions from the Earth's surface and from all levels in the atmosphere,

* Television Infrared Observation Satellite (TIROS) Operational Vertical Sounder

$$R(\nu_j) = \sum_{i=1}^{N} B[\nu_j, T(p_i)] w(\nu_j, p_i) \quad (1)$$

where

$w(\nu_j, p_i) = \varepsilon(\nu_j, p_i)\tau(\nu_j, 0 \to p_i)$ is the weighting function,

$B[\nu_j, T(p_i)]$ is the Planck radiance for pressure level *i* at temperature *T*,

$\varepsilon(\nu_j, p_i)$ is the spectral emissivity of the emitting medium at pressure level *i*,

$\tau(\nu_j, 0 \to p_i)$ is the spectral transmittance of the atmosphere above pressure level *i*.

The problem is to determine the temperature (and moisture) at *N* levels in the atmosphere from *M* radiance observations. However, because the weighting functions are broad and represent an average radiance contribution from a layer, the *M* radiance observations are interdependent, and hence there is no unique solution. Furthermore, the solution is unstable in that small errors in the radiance observations could produce large errors in the temperature profile. For this reason, the solution is approximated in a linearized form. First eq. (1) is re-written in terms of a deviation from an initial state,

$$R(\nu_j) - R_0(\nu_j) = \sum_{i=1}^{N} \left\{ B[\nu_j, T(p_i)] - B[\nu_j, T_0(p_i)] \right\} w(\nu_j, p_i) + e(\nu_j) \quad (2)$$

where

$e(\nu_j)$ is the measurement error for the radiance observation.

In order to solve eq. (2) for the temperature profile *T* it is necessary to linearize the Planck function dependence on frequency. This can be achieved since in the infrared region the Planck function is much more dependent on temperature than frequency. Thus the general inverse solution of eq. (2) for the temperature profile can be written as

$$T(p_i) - T_0(p_i) = \sum_{j=1}^{M} A(\nu_j, p_i) \left[R(\nu_j) - R_0(\nu_j) \right] \quad (3)$$

or in matrix form

$T = AR$

where A is a linear operator. Referring back to eq. (2), it can be seen that in theory *A* is simply the inverse of the weighting function matrix. However in practice the inverse is numerically unstable.

The statistical regression algorithm seeks a "best-fit" operator matrix *A* that is computed using least-squares methods by utilizing a large sample of atmospheric temperature and moisture soundings, and collocated radiance observations. That is, we seek to minimize the error

$$\frac{\partial}{\partial A} |AR - T|^2 = 0 \quad (4)$$

which is solved by the normal equation to yield

$$A = \left(R^T R \right)^{-1} R^T T \quad (5)$$

where

$\left(R^T R \right)$ is the covariance of the radiance observations,

$\left(R^T T \right)$ is the covariance of the radiance observations with the temperature profile.

Ideally, the radiance observations would be taken from actual VIIRS measurements, and used with time and space co-located radiosonde profiles to directly derive the regression coefficients *A*. In such an approach, the regression relationship would not involve any radiative transfer calculations. However, radiosondes are routinely launched only two times each day at 0000 UTC and 1200 UTC simultaneously around the earth; S-NPP passes occur at roughly 0100-0200 AM and PM local standard time each day. It is therefore not possible to obtain many time and space co-located VIIRS radiances. Alternatively, the regression coefficients can also be generated from VIIRS radiances calculated using a transmittance model with profile input from a global temperature and moisture radiosonde database. In this approach, the accuracy of the atmospheric transmittance functions for the various spectral bands is crucial for accurate parameter retrieval.

In the TPW algorithm the regression coefficients have been established by using the SeeBor Training Dataset (Borbas et al., 2005). Compared to the MOD07 method, CrIS/ATMS-based water vapor is a new predictor in the proposed method. The calculated IR window (IRW) BTs (using CRTM) and the newly added CrIS/ATMS water vapor products have been regressed against radiosonde-measured TPWs. Those regression coefficients have been applied to VIIRS IRW BTs and the CrIS/ATMS water vapor product in clear skies (as determined from the VIIRS cloud mask) to infer a TPW product at VIIRS native spatial resolution (750 m). The UW Global IR Baseline Fit Emissivity Database was used to assign the VIIRS surface emissivity required for the VIIRS BT simulation.

In the regression procedure, the primary predictors are VIIRS infrared spectral band brightness temperatures. The retrieval algorithm requires calibrated, navigated, co-registered 0.75 km FOV radiances from bands M14 to M16 (8.55, 10.7, and 12.0 μm). Estimates of surface pressure, latitude, percent land, and month are also used as predictors to improve the retrieval. Table 1 lists the predictors and their noise used in the regression procedure. Quadratic terms of all brightness temperatures are also used as predictors to account for the moisture non-linearity in the VIIRS radiances. The noise used in the algorithm is the estimate of post-launch noise. The regression coefficients are generated for 60 local zenith angles from nadir to 65° and viewing angle classifications is used to limit the retrievals to training data with physical relevance to the observed conditions. This synthetic regression technique is mature and has been widely used for sounding retrievals, including GOES sounder (Li et al., 2001), MODIS (Seemann et al., 2003), ATOVS (Li et al., 2000) and others.

Table 1: Predictors and their uncertainty used in the regression procedure

Predictor	**Noise used in VIIRS algorithm**
Band M14 (8.55μm)	0.064°K
Band M15 (10.7μm)	0.028°K
Band M16 (12.0μm)	0.036°K
Surface Pressure	5 hPa
Percentage of land	0.01
Latitude	0.1
Month	0.1

The regression coefficients are generated using the calculated synthetic radiances and the matching atmospheric profiles. To perform the regression, Eq. (5) can be applied to the actual VIIRS measurements to obtain the estimated total precipitable water. The advantage of this approach is that it does not need VIIRS radiances collocated in time and space with atmospheric profile data; it requires only historical profile observations. However, it involves the radiative transfer calculations and requires an accurate forward model in order to obtain a reliable regression relationship. Calculations of the synthetic VIIRS radiances require a

physically realistic characterization of the surface, including land surface emissivity, skin temperature and surface pressure.

Determination of the total column precipitable water vapor is performed by integrating moisture profile through the atmospheric column. The total column precipitable water vapor parameter is integrated from the 101-level retrieved mixing ratio profiles (from the surface up to the 10 hPa- level pressure level).

2.3. *Cloud Detection Algorithm*

VIIRS TPW determinations require clear sky measurements. The operational VIIRS MODIS Cloud Mask (VMCM) algorithm (Ackerman et al., 2019) is used to identify pixels that are cloud free. The VIIRS cloud mask algorithm determines if a given pixel is clear by combining the results of several spectral threshold tests. A confidence level of clear sky for each pixel is estimated based on a comparison between observed radiances and specified thresholds. The 0.95 or higher clear sky confidence has been used to determine clear scenes for the VIIRS TPW Retrievals. Since the decision to perform a retrieval depends upon the validity of the cloud mask algorithm, cloud contamination may occur if the cloud mask fails to detect a cloud, and the retrieval may not be made if the cloud mask falsely identifies a cloud.

2.4. *Regression Profile Training Data Set*

In generating the VIIRS water vapor retrieval regression coefficients, global profiles of temperature, moisture, and ozone from the SeeBor profile database (Borbas et al., 2005) are used. The SeeBor training database consists of 15,704 global profiles of temperature, moisture, and ozone at 101 pressure levels for clear sky conditions. The profiles are taken from the NOAA-88, ECMWF, and TIGR-3 training datasets, ozone sondes from eight NOAA Climate Monitoring and Diagnostics Laboratory (CMDL) sites, and global radiosondes from the NOAA Forecast Systems Laboratory (FSL) radiosonde database. The radiative transfer calculation of the VIIRS spectral band radiances is performed with CRTM transmittance model for each profile from the training data set to provide a temperature-moisture-ozone profile/VIIRS radiance pair. Estimates of the VIIRS instrument noise are added into the calculated spectral band radiances based on VIIRS post launch estimates.

To limit the retrievals to training data with physical relevance to the observed conditions, the SeeBor dataset was partitioned into four land and three ocean zones based upon the calculated 11μm brightness temperatures (BT11) as discussed in Borbas et al. (2005). These zones and BT11 temperature ranges are shown in Table 2. Each retrieval uses only a subset of the training data corresponding to the BT11 ranges with a 3K overlap. The land/ocean BT11 groups were chosen to allow for sufficient profiles in each category while keeping regions with similar surface radiative properties together.

Table 2: Brightness temperature zones used in training data and regression retrieval

Zone number	BT11 range for training (K)	BT11 range for retrievals	Number of profiles
Land			
1	< 275	< 272	1978
2	269-290	272-287	2538
3	284-299	287-296	2807
4	293-353	296-350	2226
Ocean			
1	< 286.5	< 283.5	2214
2	280.5-296	283.5-293	2900
3	290-353	293-350	2437

2.5. *Land Surface Characterization*

To calculate the synthetic VIIRS radiances, a physically realistic characterization of the surface is required. Land surface emissivity and skin temperature are assigned to each profile as described below. Surface pressure is taken from the 0.5 degree spatial resolution NOAA CFSR (Climate Forecast System Re-analysis, Saha et al., 2010), with bilinear interpolation among neighboring pixels. Global skin temperature over land is characterized as a function of surface air temperature, solar zenith angle (3 categories), and azimuth angles (8 categories). To build the relationship, surface skin temperature measurements from the infrared thermometer (IRT) at the ARM SGP site in Oklahoma were used together with surface air temperature measured by radiosonde from the period April 2001 to October 2003. The difference between the IRT-measured surface skin temperature and the radiosonde surface air temperature for 124 clear sky cases is shown as a function of solar zenith and azimuth angles in Figure 2. The relationship defined by Fig. 2 was used to assign a skin temperature to all profiles.

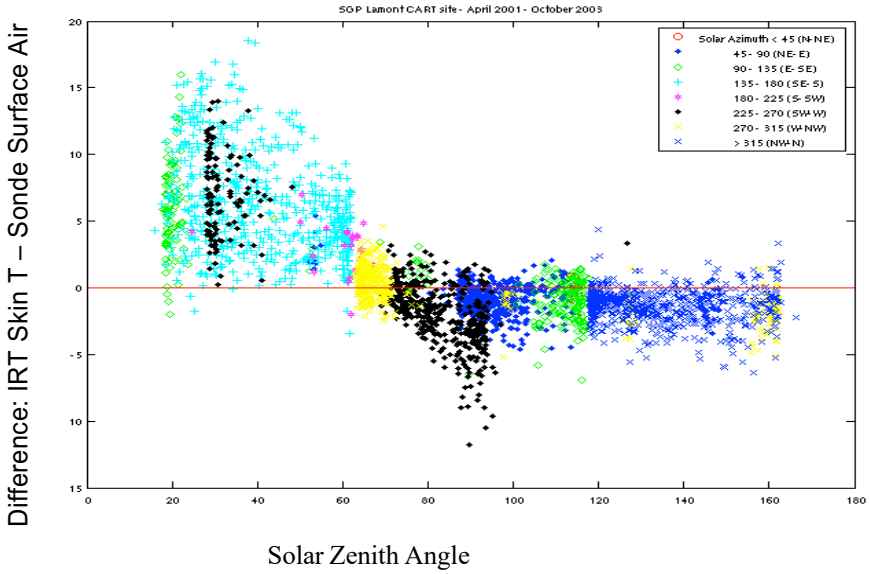

Figure 2: Skin Temperature and Surface Air Temperature relationship for the SGP CART site based on clear sky observations between April 2001 and October 2003. Points are colored according to solar azimuth category.

Land surface emissivity values are assigned to the training data profiles based on the UW Global IR Land Surface or Baseline Fit (BF) Emissivity Database. The derivation of the database and its application to the MOD07 retrieval products is described in detail in Seemann et al. (2008) and summarized here. This emissivity is derived using input from the MODIS operational land surface emissivity product (called MOD11). A procedure called the baseline fit method, based on laboratory measurements (Salisbury and D'Aria, 1992) of surface emissivity, is applied to fill in the spectral gaps between the six MOD11 wavelengths. These MOD11 wavelengths span only three spectral regions: 3.8–4 μm, 8.6 μm, and 11–12 μm, but the MOD07 retrievals require surface emissivity at higher spectral resolution. BF emissivity is available at 0.05 degree spatial resolution globally at ten wavelengths: 3.7, 5.0, 5.8, 7.6, 8.3, 9.3, 10.8, 12.1, and 14.3 μm. The ten wavelengths were chosen as inflection points to capture as much of the shape of the higher resolution emissivity spectra as possible between 3.6 and 14.3 μm, so emissivity values in between the inflection points can be found by interpolation.

2.6. Implementing the new algorithm on combined VIIRS and CrIS/ATMS data

As indicated, a clear sky regression relationship is established between TPW and VIIRS IRW BTs (in 8.6, 10.8, and 12 μm) and NUCAPS water vapor soundings calculated from a global training radiosonde-based profile data set. The VIIRS cloud mask is used to indicate cloudy VIIRS FOVs. The NUCAPS retrievals are smoothed using a radius of 60 VIIRS pixels. First the VIIRS-only clear sky TPW is generated, and then the VIIRS+NUCAPS TPW is calculated in clear skies when NUCAPS has determined a TPW (holes exist when surface emissivity or other issues interfere with a NUCAPS retrieval). The remaining holes in the VIIRS+NUCAPS TPW field are filled with adjusted VIIRS-only or adjusted NUCAPS-only TPWs. The adjustment process for the given 6-minute granule consists of constructing a linear fit of the VIIRS+NUCAPS TPW against collocated the VIIRS-only TPW; another linear fit is determined for the VIIRS+NUCAPS TPW against collocated NUCAPS-only TPW. The appropriate linear fit is then used to scale the VIIRS-only TPW and the NUCAPS-only TPW to fill holes where possible. The resulting TPW field shows more detail than VIIRS alone, NUCAPS alone, and MODIS alone. The NUCAPS-alone holes due to surface emissivity issues are filled by using VIIRS-only values and holes in VIIRS-only due to interference in non-precipitating clouds are filled by using smoothed NUCAPS values. Figure 3 shows the comparisons for a granule on October 15, 2015 at 08:50 UTC.

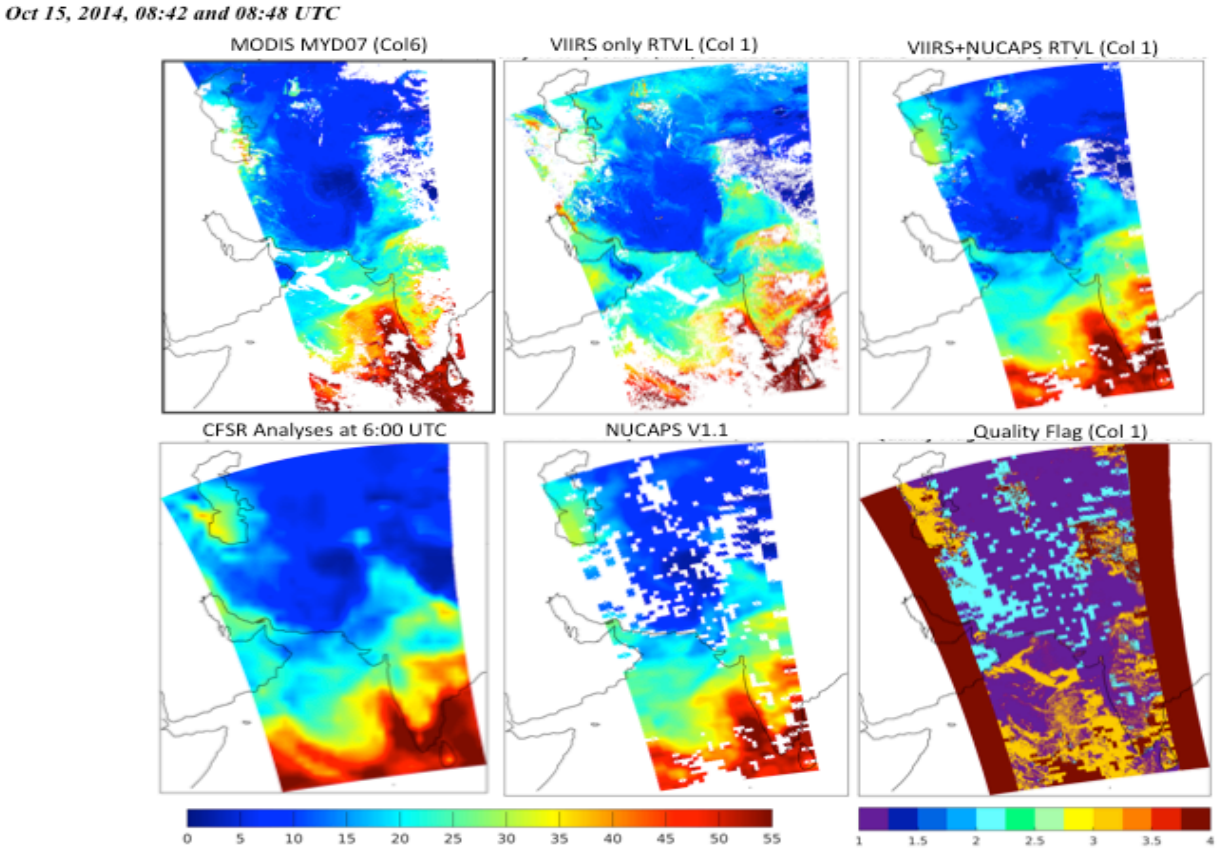

Figure 3: TPW comparison on 15 October 2015 at ~850 UTC: (top left) Aqua MODIS, (top middle) VIIRS only, (top right) VIIRS plus NUCAPS with holes filled by adjusted VIIRS-only or smoothed NUCAPS-only values, (bottom right) CFSR re-analyses, (bottom middle) NUCAPS-only, and (bottom right) the WATVP Level-2 quality flag. Notice the better coverage and improved values of VIIRS plus NUCAPS with holes filled over VIIRS-only, NUCAPS-only, and even MODIS.

The input data files of the S-NPP VIIRS Water Vapor Level-2 (WATVP_L2_VIIRS_SNPP algorithm are:

1. The VIIRS L1B data file in the SIPS Internal File Format (IFF)
2. VIIRS Cloud Mask (MVCM) file
3. NUCAPS TPW product file
4. Collocation file between VIIRS L1B and the CrIS/ATMS (NUCAPS) resolution (using collopak)
5. The CFSR Re-analyses for surface pressure

The latest version of the input files and software required to process them are listed in Table 3a,b.

The 750m resolution outputs included in the 6-minute WATVP_L2_VIIRS_SNPP output file:

Geophysical data:

- *atmosphere_water_vapor_content_nucaps_bg (collocated NUCAPS retrieval)*
- *atmosphere_water_vapor_content_viirs_nucaps (VIIRS+NUCAPS retrieval)*
- *atmosphere_water_vapor_content_viirs_only (VIIRS-only retrieval)*
- *surface_skin_temperature*
- *quality_flag*
  - *1 = good retrieval-VIIRS and NUCAPS data are available;*
  - *2 = filled with VIIRS-only retrieval;*
  - *3 = filled with NUCAPS-only retrieval;*
  - *4 = No retrievals - no VIIRS nor NUCAPS data are available or non-physical retrievals*
- *model_atmosphere_water_vapor_content (from CFSR file)*
- *model_surface_pressure (from CFSR file)*
- *clear_sky_confidence (from the VMCM file)*

Geolocation data:

- *land_sea_mask,*
- *latitude,*
- *longitude,*
- *sensor_zenith,*
- *solar_zenith*

The algorithm contains a sanity check by filtering out the 90 mm or higher water vapor products (viirs_only, nucaps_bg and viirs_nucaps) and also has a constraint for the VIIRS-only and NUCAPS-only (nucaps_bg) retrievals to be inside the minimum and maximum values of the granule. Figure 4 and Tables 3 a/b summarize the latest SIPS process flow with up-to-date version number of the inputs.

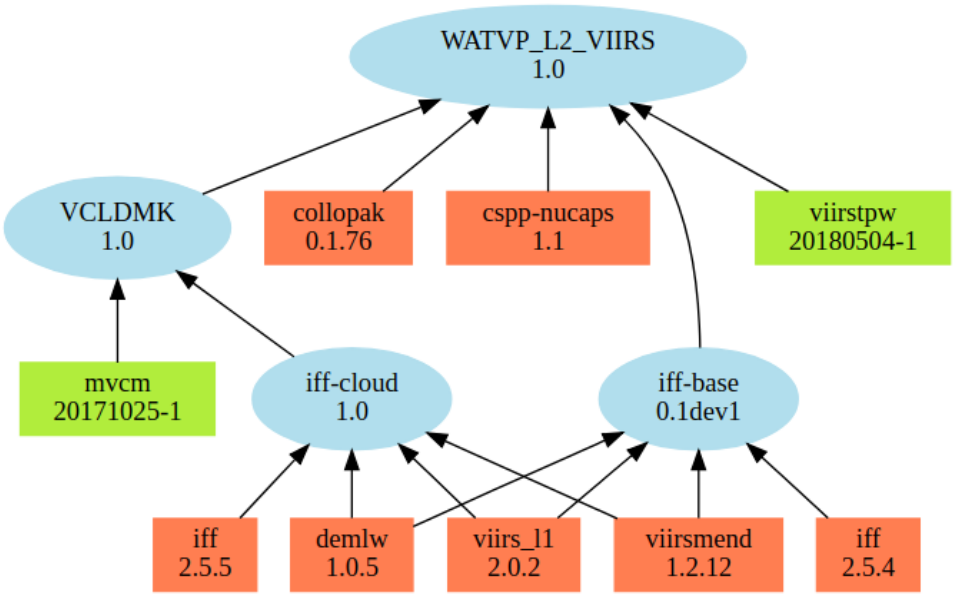

Figure 4: Input data flow of the S-NPP VIIRS TPW processing with the indication of the data version numbers.

Table 3a: Direct inputs required directly by the WATVP product.

Name	Package	Type
VIIRS TPW software	viirstpw: 20180504-1	delivery
Collocation data	collopak: 0.1.76	support
IFF: base config	iff-base: 0.1dev1	product
VIIRS Cloud Mask	VCLDMK: 1.0	product
CSPP NUCAPS	cspp-nucaps: 1.1	support

Table 3b: Indirect inputs not directly required by the product but part of the input graph.

Name	Package	Type
Land-water mask generation	demlw: 1.0.5	Support
VIIRS L1B bowtie restoral	viirsmend: 1.2.12	Support
NASA VIIRS Level 1	viirs_l1: 2.0.2	Support
Intermediate File Format	iff: 2.5.5	Support
MODIS/VIIRS Cloud Mask	mvcm: 20171025-1	Delivery
IFF: Cloud Team Config	iff-cloud: 1.0	Product

3. The Level-3 daily and monthly mean products

Level-3 global 0.5° by 0.5° daily and monthly mean data products (called WATVP_D/M3_VIIRS_SNPP) were developed by using a gridding software (called Yori) developed at UW-Madison SSEC (Veglio et al., 2018) and implemented on the NASA VIIRS Atmosphere SIPS. Yori has been adapted for the VIIRS TPW products and has been processed on the WATVP_L2_VIIRS_SNPP (1.0dev4) data.

The Level-3 processing workflow using the Yori software is structured in five separate steps:

1. Preparing the YAML file (configuration file for our products)
2. Preparing the transitional/intermediate input netCDF files (*preyori.py*)
3. Gridding the Level-2 input granule (*rungrid.py*, see Fig 5a)
4. Aggregating a day (*yori_aggregate.py*)

5. Aggregating a month (*yori_aggregate.py*, see Fig 5b).

The mean and standard deviation are calculated for each grid cell, and the sum, the square of the sum, and number of pixels in the cells are also stored in the Level-3 (daily and monthly) output files for further aggregation purposes.

The data can be filtered by a given mask specified by the users. For the WATVP_D/M3 products, only the day/night mask was used based on the solar zenith angle. The pixels having solar zenith angle less than 95 degrees are considered as "day" while solar zenith angle more than 95 degrees are considered as "night."

The output products included in the WATVP_D/M3_VIIRS_SNPP product file are:

group: night_atmosphere_water_vapor_content_viirs_nucaps (VIIRS+NUCAPS retrieval)
variables: standard_deviation, sum, sum_squares, n_points, mean
group: night_atmosphere_water_vapor_content_ nucaps_bg (NUCAPS retrieval)
variables: standard_deviation, sum, sum_squares, n_points, mean
group: night_atmosphere_water_vapor_content_viirs_only (VIIRS-only retrieval)
variables: standard_deviation, sum, sum_squares, n_points, mean
group: day_atmosphere_water_vapor_content_viirs_nucaps (VIIRS+NUCAPS retrieval)
variables: standard_deviation, sum, sum_squares, n_points, mean
group: day_atmosphere_water_vapor_content_nucaps_bg (NUCAPS retrieval)
variables: standard_deviation, sum, sum_squares, n_points, mean
group: day_atmosphere_water_vapor_content_viirs_only (VIIRS-only retrieval)
variables: standard_deviation, sum, sum_squares, n_points, mean

Figure 6 illustrates the results of step 3 in the process, when the L2 VIIRS TPW granule products (Fig 6 top panels) have been converted into the corresponding 0.5° resolution gridded products (Fig 6 bottom panels). As an example, the L3 daily and monthly aggregated products have been shown in Figure 7 for Oct 15, 2014 and Oct 2014 respectively, and compared to the MYD08 products. Please note the better coverage, due to 1) using the all sky NUCAPS TPW products and 2) filling with modified NUCAPS-only or VIIRS-only TPW values.

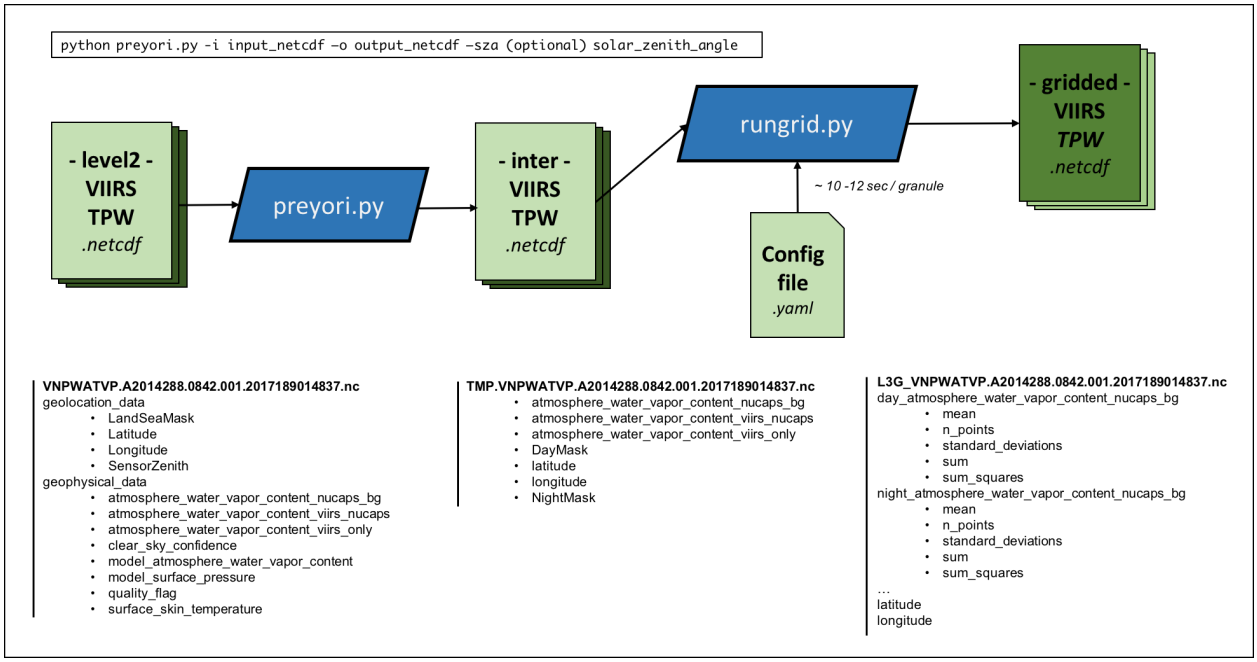

Figure 5a: Work flow of VIIRS TPW L3 Processing (steps 1-3) to create L3 gridded granule products.

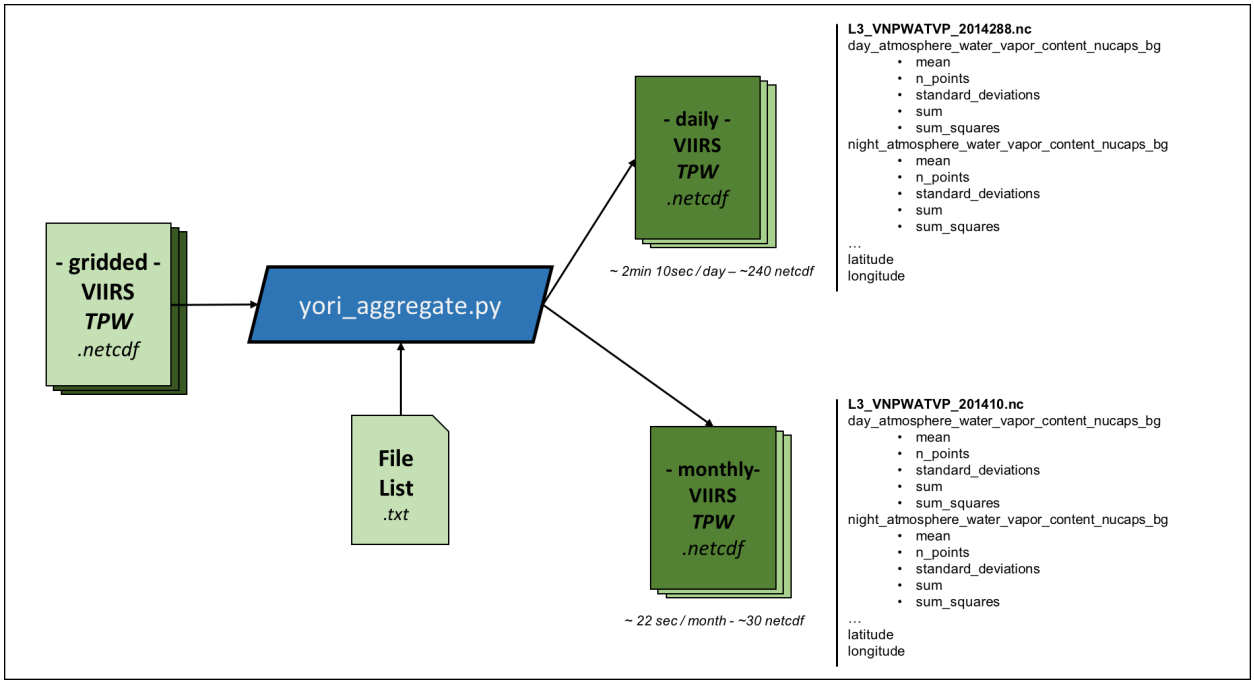

Figure 5b: Work flow of VIIRS TPW L3 Processing (steps 4-5) to create L3 gridded daily and monthly mean products.

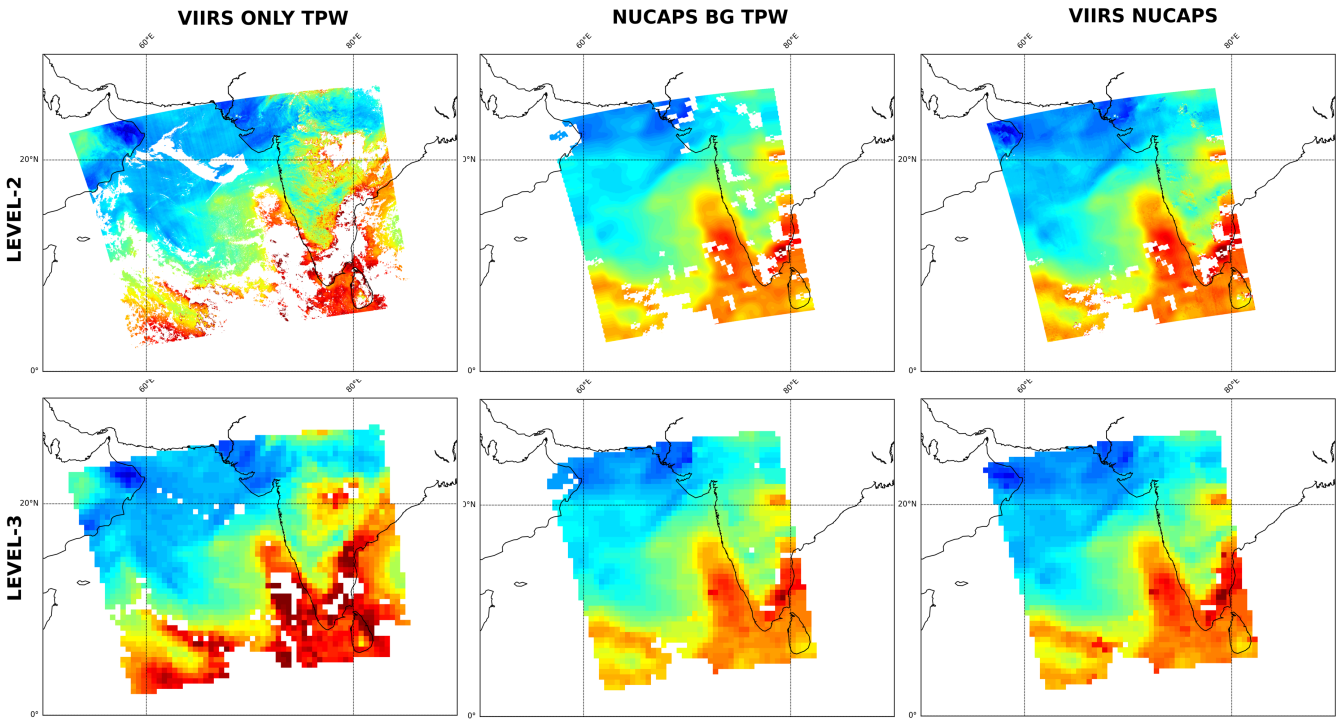

Figure 6. Processing a VIIRS TPW granule (top) to a gridded granule (bottom) on 15 October 2014 at ~08:50 UTC. VIIRS-only (left), NUCAPS background (middle) and VIIRS+NUCAPS (right) TPW fields are shown.

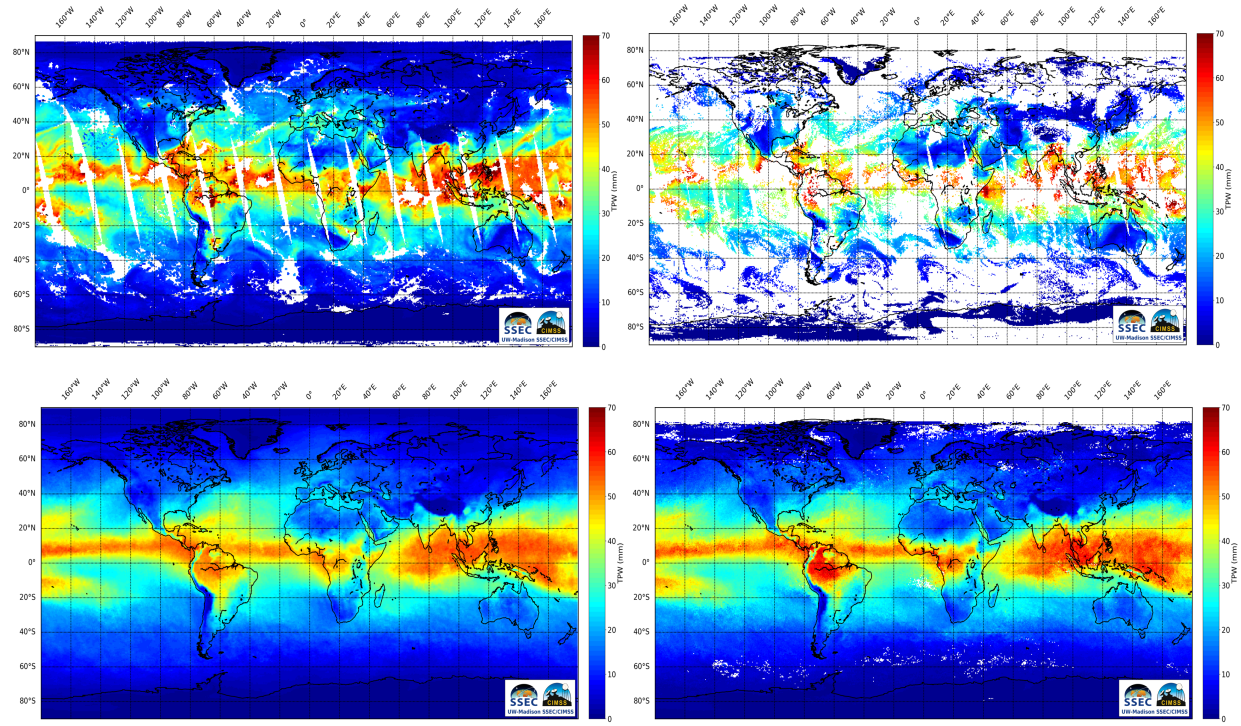

Figure 7: Daytime daily (Oct 15, 2014, top panels) and monthly (Oct 2014, bottom panels) mean 0.5 degree gridded VIIRS/NUCAPS (left) and AQUA/MODIS MYD07 (right) TPW products.

4. Validation of the WATVP L2 products

The WATVP level-2 TPW products have been validated with *in situ* measurements such as the Microwave Radiometer (MWR), GPS TPW, and satellite-based TPW retrievals derived from MODIS, AIRS+AMSU, and CrIS+ATMS measurements. This section describes the validation method and results.

4.1. Validation data and their availability

Total precipitable water measurements were collected from 2012 January to 2015 July over the Atmospheric Radiation Measurement (ARM) Southern Great Plain (SGP, Lat: 36° 36'N, Lon:97° 29') Cloud and Radiation Testbed (CART) site. The MWR and GPS data (from the Suomi Network, Ware et al., 2000) were downloaded from the ARM data discovery website (http://www.archive.arm.gov/discovery/#v/home/s/).

MODIS MYD07 Level-2 TPW retrievals were downloaded over the SGP CART site where MWR data was available from the LAADS Web site (https://ladsweb.nascom.nasa.gov/data/search.html), by choosing about +/- 0.5 degree area around the site coordinates, and the minimum successful retrieval percentage was set to 70%.

AIRS and AIRS+AMSU data files were obtained from the Mirador data holdings (http://mirador.gsfc.nasa.gov/) for the CART site.

The NUCAPS data files were downloaded from the NOAA CLASS website (http://class.noaa.gov), based on the Suomi-NPP satellite overpass times.

VIIRS retrievals were selected for the SGP site also based on a list of the satellite overpass times using the NASA Atmosphere SIPS OrbNav online tool. The VIIRS-like MODIS retrievals were processed in-house. These retrievals use only the 3 MODIS bands which are similar to the VIIRS 8.6, 10.8 and 12 μm bands to simulate VIIRS. These retrievals were processed for the SGP CART site overpasses only. GPS data was collected for the SGP site within one hour. Figure 8 shows the time series of all the collected data except the AIRS L2 products.

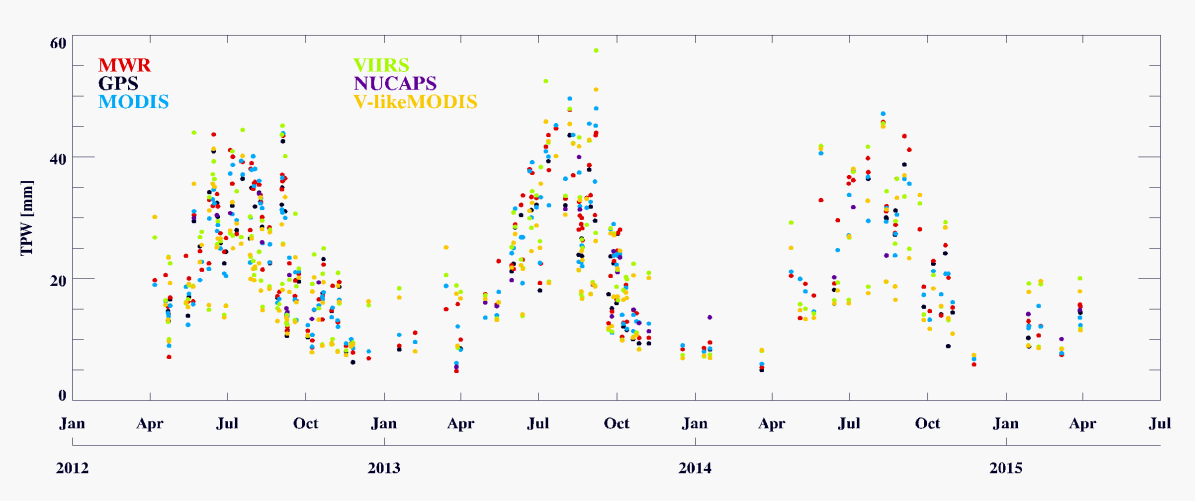

Figure 8: Collocated VIIRS, VIIRS-like MODIS, MODIS, NUCPAS, GPS and MWR TPW data at SGP CART site between 2012 January and 2015 July.

4.2. Collocations

VIIRS, VIIRS-like MODIS, MYD07, NUCAPS (CrIS+ATMS), and AIRS L2 TPW retrievals have been collocated in time and space with the MWR and GPS data at the SGP CART site.

For VIIRS, VIIRS-like MODIS and MYD07 TPW retrievals, the closest pixel was selected. If the closest pixel within 5 km was clear, a 20 km radius area was selected for further analysis. If more than 90% of the pixels in this circle-shaped area were clear, the average and standard deviation was calculated and assigned to that site.

The horizontal spatial resolution of NUCAPS and AIRS L2 data is around 50 km, hence no spatial averaging was done, the closest pixel to the site was selected. Since the NUCAPS files do not contain the TPW product, it has been integrated from the mixing ratio profiles by using surface pressure to define the surface level. Quality flag was taken into account; just the 'accepted' values were used. In order to select only the clear cases the 'Cloud Top Fraction' variable was used. This contains information for 8 cloud levels and gives a number between 0-1 or missing value. In our approach only those pixels were taken into account where the maximum of the Cloud Top Fraction through the layers was less than 0.2 (Using zero as a threshold gave very few cases). The AIRS L2 products contain quality information about the TPW product (0: perfect; 1: good; 2: do not use). Only the perfect and good quality data were used in this comparison.

Figure 9 shows an example of the collocation method for MODIS on 22 May 2015 at 19:55 UTC around the SGP CART site (black star on the top map). Bottom panels of Figure 9 show the surrounding area around the site, the 20 km radius area and the calculated average for this circle.

For time matching with the 30-sec MWR data, the time of the collocated pixel of each type of TPW retrievals was selected from the MWR time series and the surrounding 5 minutes of data was averaged. It includes about 10-15 MWR measurements (see Fig. 10).

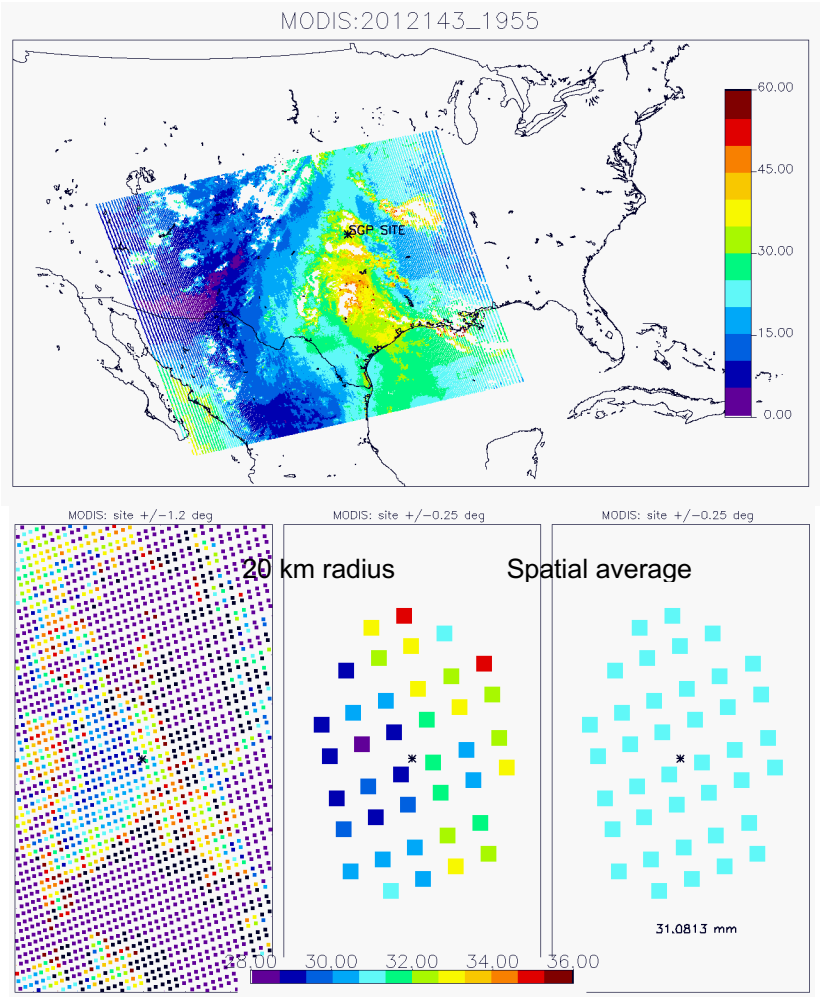

Figure 9: (top) MODIS TPW on 22 May 2015 at 19:55 UTC around the SGP_C1 CART site (black star). (bottom) the surrounding area around the SGP Cart site (left), the 20 km radius area (middle) and the calculated average for this circle (right).

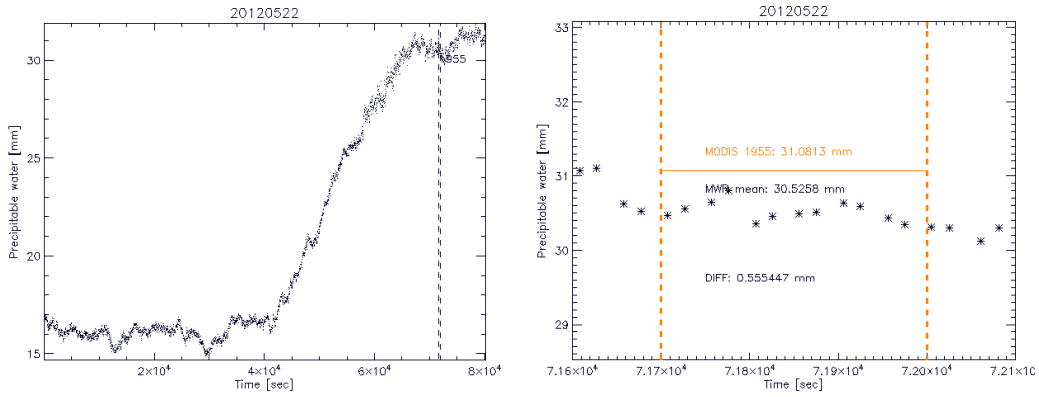

Figure 10: MWR TPW values on 22 May 2015. Left figure shows the TPW time-series for the whole year, right figure illustrates the time collocated TPW values during the MODIS granule (19:55UTC-20:00 UTC). Red vertical dashed lines show the beginning and end time of that 5-minute granule.

4.3. Evaluation

As a next step, statistical measures of the collocated data were calculated, such as bias, standard deviation, root mean square error, and correlation.

Figures 11 and 12 illustrate an example granule to evaluate the VIIRS+NUCAPS TPW retrievals on October 15, 2014 at 19:00 UTC. The new VIIRS+NUCAPS TPW product shows more accurate TPW values, than the VIIRS-only one. The difference at the SGP CART site was 5.8 mm in case of VIIRS-only, but for VIIRS +NUCAPS it is only 1.5 mm (Fig. 12). Note that, the image of VIIRS+NUCAPS TPW (right panel of Figure 11) has been processed without smoothing the input NUCAPS TPW product. The time series of the VIIRS+NUCAPS TPW retrievals vs MWR collocation set and their statistical comparisons are plotted in Figure 13.

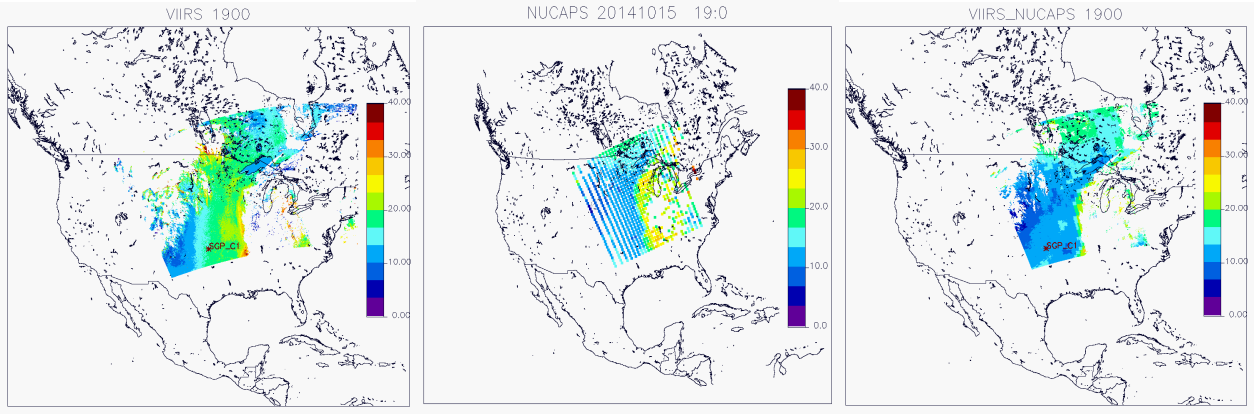

Figure 11: TPW retrieval results on 15 October 2014 at 19:00UTC). VIIRS-only (left) and NUCAPS-only (middle) and the VIIRS+NUCAPS TPW (right) retrievals (before filling up the gaps and smoothing NUPCAPS retrievals). The location of the SGP site is indicated with a star.

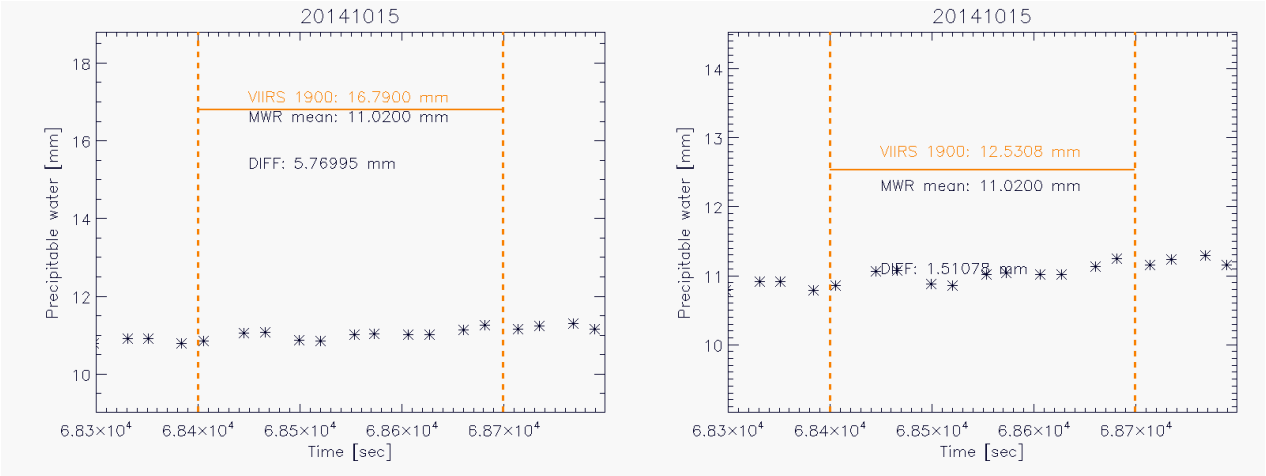

Figure 12: Time series of the TPW Retrievals derived from VIIRS-only (left) and VIIRS+NUCAPS (right), and comparison to MWR values (black stars) at the SGP site for 15 October at 19:00. (note: different scales in the diagram)

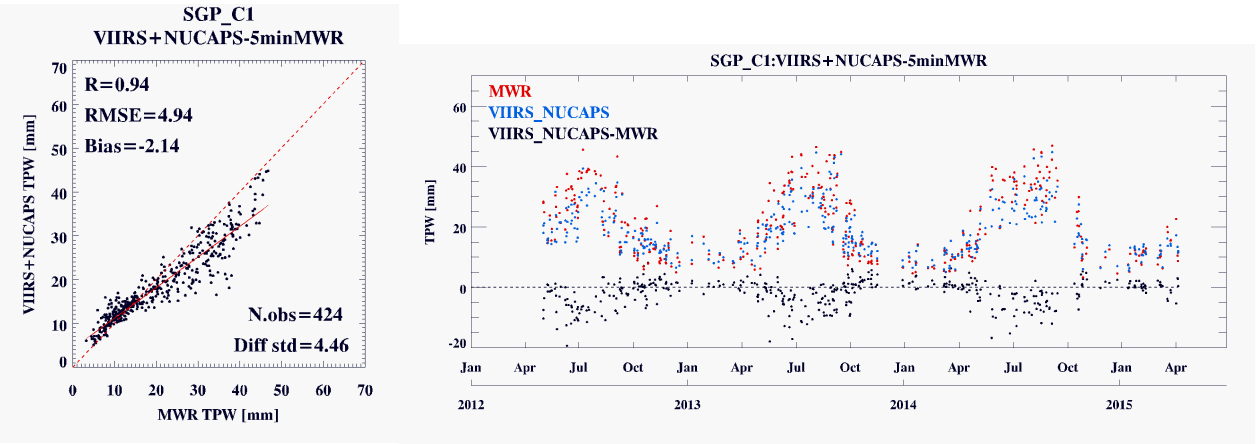

Figure 13: VIIRS+NUCAPS TPW retrievals vs MWR collocation for the SGP site. (left) Scatterplot and statistics of the comparison, (right) time-series of the two TPW data (MWR: red and VIIRS+NUCAPS: blue) and their differences (black) are plotted.

Table 4 summarizes all the statistical results between the available TPW retrievals and MWR TPW over the SGP Cart site. As expected, the VIIRS-only TPW product has a similar quality as the simulated VIIRS-like MODIS product. When the NUCAPS TPW is added to the VIIRS-only retrievals, the bias and standard deviation, and hence the RMS difference of the VIIRS+NUCAPS products was reduced, and the correlation was increased. The statistical characteristics of the new products became similar to the MODIS MYD07 TPW products.

Table 4: Statistical comparison of TPW derived from MODIS, VIIRS-like MODIS, VIIRS-only, NUCAPS, GPS, AIRS-only and AIRS+AMSU L2 products and the combined VIIRS+NUCAPS retrievals. Bias, standard deviation, root mean square differences and correlation are calculated between the TPW retrievals and MWR TPW measurements over the SGP Cart site.

	MODIS	VIIRS-like MODIS	VIIRS	NUCAPS	VIIRS+ NUCAPS	GPS	AIRS L2	AIRS +AMSU L2
nsamples	345	344	697	426	424	47205	548	524
bias	-1.25	-2.36	-1.65	-0.93	-2.14	1.14	-1.23	-1.17
RMSE	4.72	7.95	7.96	4.16	4.94	1.91	3.92	3.98
STDEV	4.56	7.61	7.8	4.06	4.46	1.54	3.72	3.81
Correlation	0.92	0.75	0.73	0.95	0.94	0.99	0.96	0.95

5. Evaluation of the WATVP L3 products

The L3 VIIRS TPW daily and monthly mean products have been evaluated between May 2012 and Dec 2016 with the NUCAPS, AIRS L3, Aqua/MODIS MYD08, the in-house Aqua/MODIS MYD07_L3 and the SSMI products (see Table 5 and section 6.1 Data References for more details about these datasets).

Table 5 TPW Products used for the zonal cross comparison

TPW data products		Res.
VIIRS	VIIRS-Only (day / night)	0.5 °
CrIS+ATMS	NUCAPS BG (day / night)	0.5 °
VIIRS + NUCAPS	VIIRS NUCAPS (day / night)	0.5 °
AIRS3STM	TotH2OVap_A, TotH2OVap_D	1 °
MYD08_M3	Atm. Water Vapor	1 °
MYD07_L3	TPW (day / night)	0.5 °
SSMI	TPW	1 °

The TPW comparison between the different products has been classified by land/sea and day/night. The land/sea mask has been calculated from the average of the monthly mean SSMI TPW products between May 2012 and December 2016. The SSMI data product contains measurements only over ocean. Over land, it given a value of -999, while over ice the pixel value is -500. The pixel values greater than zero give a good indication of the ocean, hence they have been converted into the land/sea mask. The day/night classification is defined by the solar zenith angle. The pixels having solar zenith angle less than 95 degrees are considered day while solar zenith angle more than 95 degrees are defined as night.

The time series of the mean monthly TPW products have been illustrated for the Mid-North Latitudes (30°N – 60°N) on Fig 14a, for Tropical latitudes (30°S – 30°N) on Fig 14b, and for Mid-South Latitudes (30°N – 60°N) on Fig. 14c for the 2012 May – 2016 December time period separately by day and night and land and ocean. The TPW products are: VIIRS-only (yellow), NUCAPS-only (green), VIIRS+NUCAPS (red), AIRS L3 ascending/descending (light blue), Aqua/MODIS MYD08 (grey), inhouse Aqua/MODIS MYD07_L3 (black), and SSMI (darker blue).

Generally, the WATVP VIIRS+NUCAPS combined product agrees with all the other types of TPW products very well. Additionally, all the TPW products have a very similar seasonal pattern and all agree within 3mm except the VIIRS-only product. The VIIRS-only TPW product over ocean has a smaller seasonal variation between summer and winter producing smaller maximum and larger minimum values except over land daytime for Tropical and South-Mid latitudes when the VIIRS-only TPW values are systematically higher with a bias of 3-4 mm over all other products. It has a negative bias (~4mm) over Tropical land for night case. This strong scene temperature dependence indicates the obvious lack of the VIIRS water vapor channels.

The SSMI (over ocean only) and the nighttime (descending) AIRS retrievals have about 4mm higher values than all the other IR-derived products due to the microwave instrument's nature, which is able to sense the water vapor content in cloudy conditions as well.

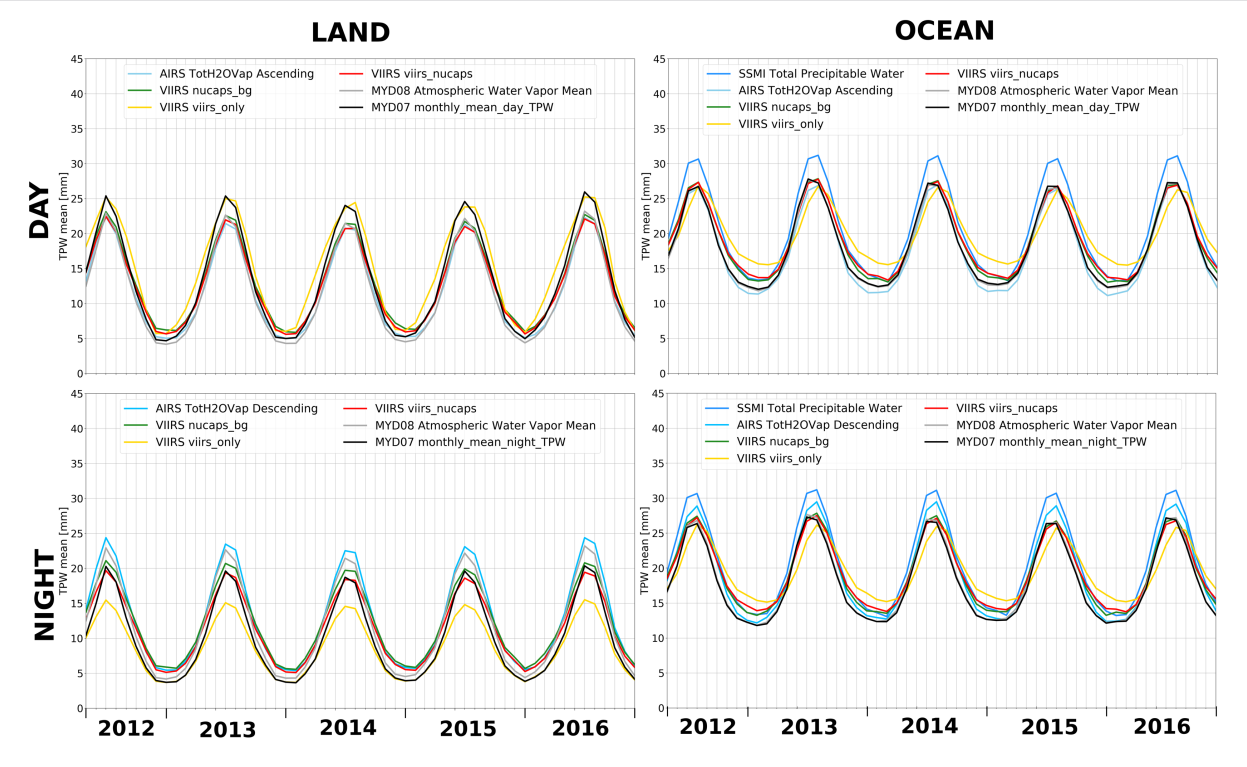

Figure 14a: The cross-comparisons of time series of different mean monthly TPW products for the **Mid-North Latitude (30°N – 60°N)** between May 2012 and December 2016. The TPW products are: VIIRS-only (yellow), NUCAPS (green), VIIRS+NUCAPS (red), AIRS L3 ascending/descending (light blue), Aqua/MODIS MYD08 (grey) , inhouse Aqua/MODIS MYD07_L3 (black) and SSMI (darker blue).

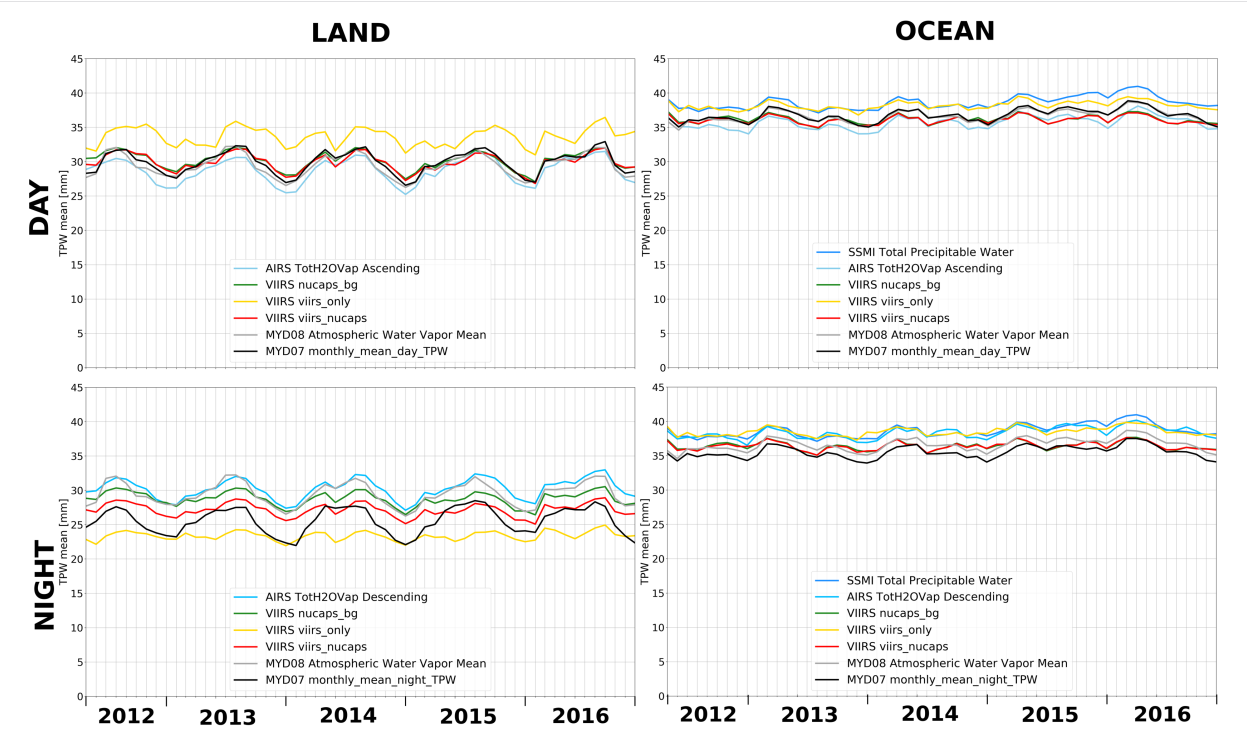

Figure 14b: Same as Figure 14a, but for the **Tropical Latitudes** (30°S – 30°N).

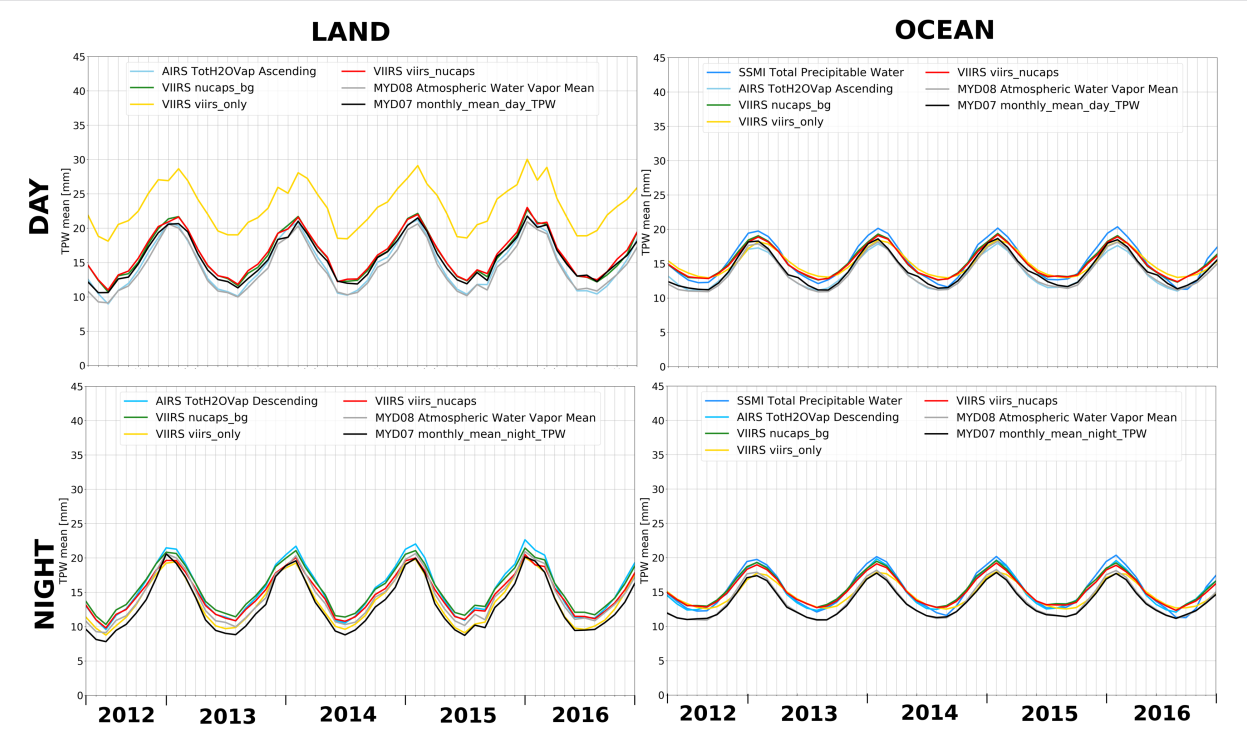

Figure 14c: Same as Figure 14a but for the **Mid-South Latitudes** (60°S – 30°S).

5.1. Comparison with Aqua/MODIS TPW

The VIIRS TPW monthly mean products (NUCAPS_bg background, VIIRS-only and VIIRS+NUCAPS) have been compared to the in-house processed MYD07 L3 monthly mean TPW product separated by day/night and land/ocean between 2012-2016. Figure 15 shows the scatter plots with RMSE error and correlations. The VIIRS+NUCAPS combined TPW product has the highest correlation with the MYD07_L3 product and the lowest RMSE errors, 2.3mm for ocean and 2.7mm for land respectively.

The temporal distribution of the correlation between the three different VIIRS TPW products and MYD07_L3 is demonstrated in Figure 16. All three products have shown the lowest correlations with the MYD07 L3 TPW products over land, summer daytime. Overall, the VIIRS-only product is the least and the VIIRS+NUCAPS product is the best fit to the MYD07 L3 TPW products. The VIIRS+NUCAPS combined TPW algorithm produces near-MODIS quality TPW in this comparison between 2012-2016 with r^2 values greater than 0.95 over land and ocean, both day and night.

The Level-2 and Level-3 comparison with Aqua MODIS reveals that VIIRS+NUCAPS TPW is a better continuation of MODIS TPW product than VIIRS- or NUCAPS-only. Besides, the VIIRS+NUCAPS TPW product has a better spatial resolution of 750m than the MODIS one at 5km. Values missing in the NUCAPS-only due to failed retrievals are filled by using VIIRS-only values. Values missing in VIIRS-only and MODIS-only due to interference by clouds are filled by using NUCAPS values. Both VIIRS-only and NUCAPS- only values are modified to reduce biases before filling in.

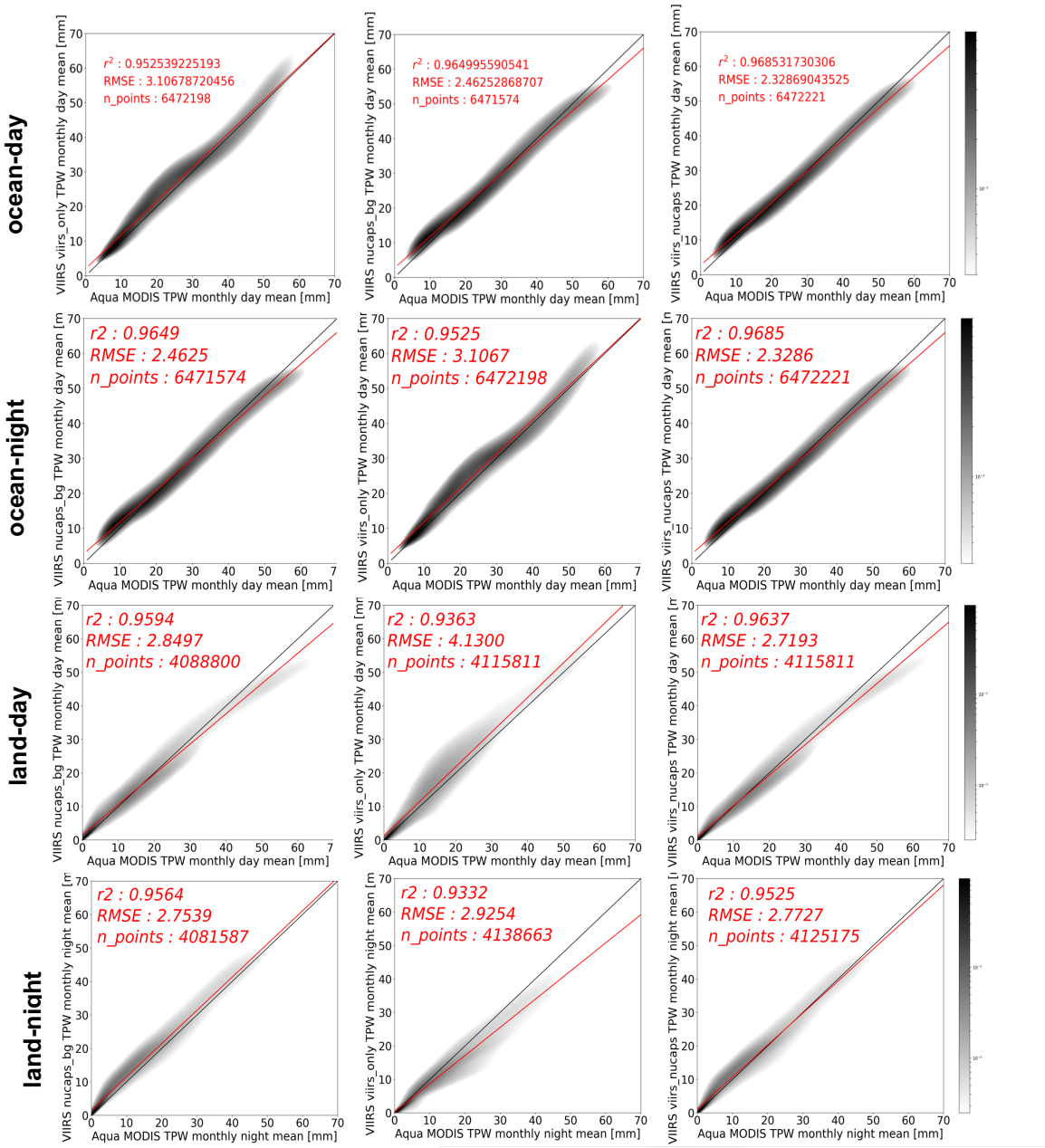

Figure 15: The scatter plots show the day, night, ocean and land separated relationship between the Level-3 MYD07 (x-axis) and the Level3 NUCAPS (left column), VIIRS-only (middle column), and VIIRS+NUCAPS (right column) data products.

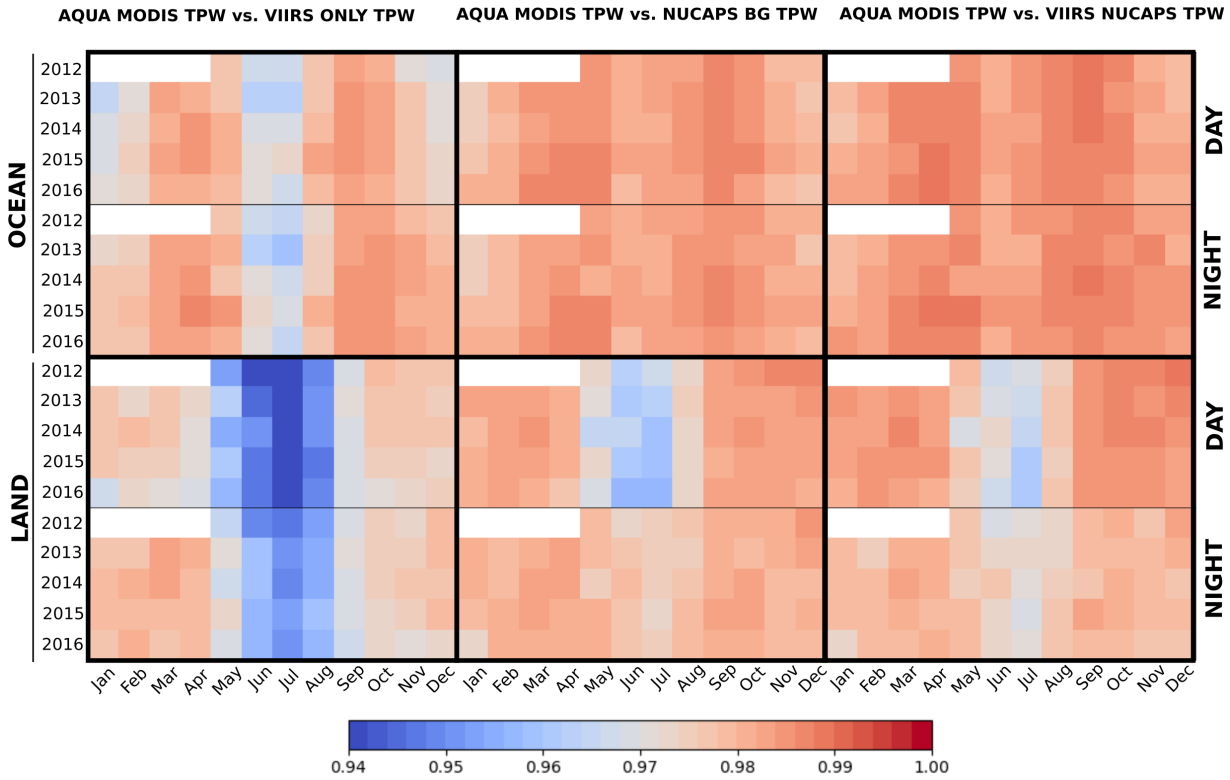

Figure 16: The correlation table shows the relationship between the Aqua MODIS and VIIRS-only (left blocks), NUCAPS (middle blocks) and VIIRS+NUCAPS (right) monthly mean Level-3 data products, separated by day, night, ocean and land.

6. Conclusion and Future Plans

This paper presents the theoretical basis, the technical aspects of the implementation and evaluation of the Level-2 and Level-3 Suomi-NPP VIIRS Water Vapor products, called WATVP_L2_VIIRS_SNPP and WATVP_D/M3_VIIRS_SNPP. The algorithm described provides total column water vapor (TPW) properties from merged VIIRS infrared measurements and CrIS plus ATMS water vapor soundings and attempts to continue the depiction of global moisture at high spatial resolution started with MODIS. While MODIS has two water vapor channels within the 6.5 μm H_2O absorption band and four channels within the 15 μm CO_2 absorption band, VIIRS has no channels in either IR absorption band. Instead, VIIRS has only three infrared window bands (8.55, 10.7, and 12 μm) with limited sensitivity to the low-level moisture (which constitutes much of the total column amount). To compensate the absence of the VIIRS water vapor channels, the NUCAPS (CrIS+ATMS) water vapor has been added to the WATVP regression algorithm. The Level-2 6-minute and 750 m spatial resolution WATVP product file includes the collocated NUCAPS background TPW, the VIIRS-only TPW, and VIIRS+NUCAPS TPW with a quality flag. Level-3 global 0.5° daily and monthly mean data products were developed using a gridding software called Yori. The Level-3 VIIRS TPW products are daily and monthly means aggregated to 0.5 degree spatial resolution separated by day and night.

The Level-2 products have been evaluated over the SGP Cart Site with MWR and other satellite-derived TPW products. VIIRS-only TPW products are similar to the VIIRS-like MODIS product (using only VIIRS- like bands for TPW retrievals). When the NUCAPS TPW is added to the VIIRS-only retrievals, the bias and

standard deviation, and hence the RMS difference of the VIIRS+NUCPAS products is reduced with a higher correlation. The statistical characteristics of the new products became similar to the MODIS MYD07 TPW products.

The Level-3 product comparison with Aqua MODIS showed that VIIRS+NUCAPS TPW quality is better than VIIRS- or NUCAPS-only. Values missing in the NUCAPS-only due to failed retrievals are filled by using VIIRS-only values. Values missing in VIIRS-only due to interference by clouds are filled by using smoothed NUCAPS values. The VIIRS+NUCAPS combined TPW algorithm produces near-MODIS quality TPW in our comparison between 2012-2016 with r^2 values greater than 0.95 over land and ocean, both day and night.

Recent developments indicate that there is the potential to generate supplementary broadband radiances at imager resolution from sounder measurements using a fusion approach (Weisz et al., 2017). In this approach, CrIS radiances are convolved with VIIRS spectral response functions and mapped to the VIIRS spatial resolution with the fusion approach. It offers the possibility of adding more information to the VIIRS+NUCAPS TPW derivation. Figure 17 shows a comparison of the VIIRS-only, VIIRS plus NUCAPS, VIIRS plus fusion radiances, and VIIRS plus NUCAPS plus fusion radiances.

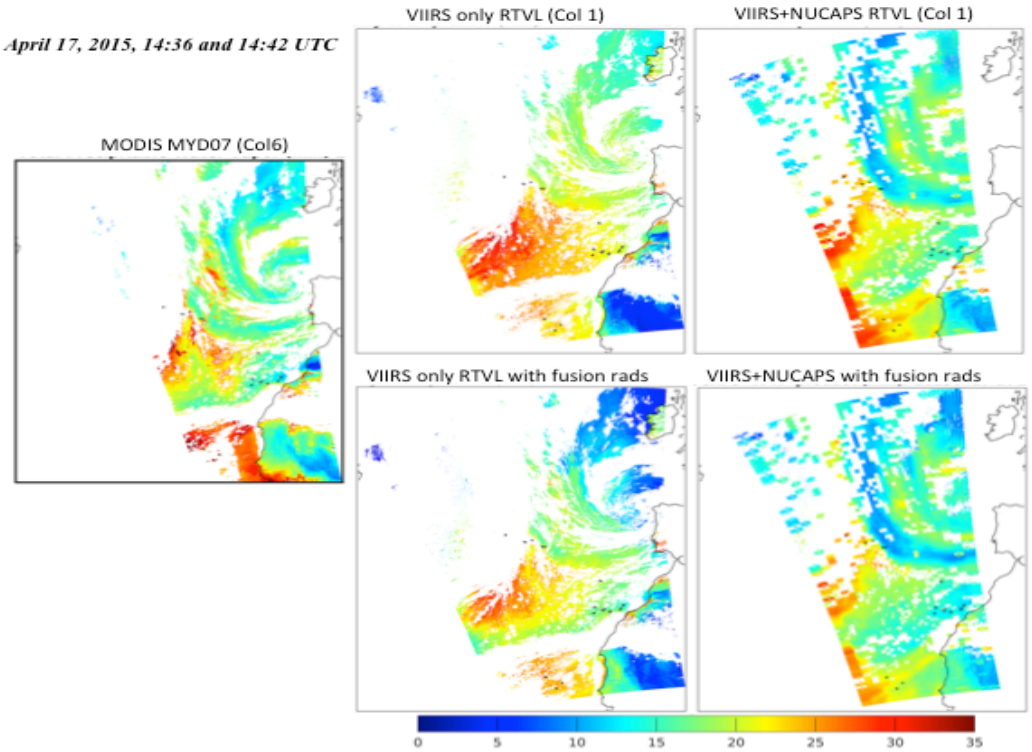

Figure 17: TPW comparison on April 17, 2015 at ~1440 UTC. (left) Aqua MODIS MYD07. (top left) Collection 1 VIIRS-only (top right) Col 1 VIIRS plus NUCAPS retrievals. (bottom left) VIRS-only (bottom right) VIIRS plus NUCAPS retrievals with MODIS-like B27 and B28 fusion channels added.

In the VIIRS regression algorithm, the radiative transfer calculation of the VIIRS emissive spectral band radiances is performed using the JCSDA CRTM model. Switching to another forward model called Radiative Transfer for TOVS (RTTOV, Saunders, et al., 2018, https://nwpsaf.eu/site/software/rttov/) offers much broader application and user support.

It remains to investigate the VIIRS-only retrieval noise (spiky TPW values) that occurs mostly over land at the edge of the clouds (not shown). The noise over land suggests it might be emissivity related. For IR emissivity estimation, the current VIIRS algorithm uses the UW Baseline Fit Emissivity Database (Seemann et al., 2008). As part of a NASA MEaSUREs project, an update of the UW emissivity database has been developed by combining it with the JPL-developed ASTER Global Emissivity Database V4 (Hulley and Hook, 2016). The new, improved Combined ASTER MODIS Emissivity Over Land (CAMEL) (Simon et al., 2018, Borbas et al., 2018) is integrated as part of the RTTOV Version-12 (Borbas et al., 2019), which makes it easy to update emissivity.

7. References

Ackerman, et al., VIIRS/SNPP Cloud Mask and Spectral Test Results 6-min L2 Swath 750m, Version-1. NASA Level-1 and Atmosphere Archive & Distribution System (LAADS) Distributed Active Archive Center (DAAC), Goddard Space Flight Center, USA, https://dx.doi.org/10.5067/VIIRS/CLDMSK_L2_VIIRS_SNPP.001

Borbas, E., S. W. Seemann, H.-L. Huang, J. Li, and W. P. Menzel, 2005: Global profile training database for satellite regression retrievals with estimates of skin temperature and emissivity. *Proc. of the Int. ATOVS Study Conference-XIV*, Beijing, China, 25-31 May 2005, pp763–770.

Borbas, E.E.; Hulley, G.; Feltz, M.; Knuteson, R.; Hook, S. 2018: The Combined ASTER MODIS Emissivity over Land (CAMEL) Part 1: Methodology and High Spectral Resolution Application. *Remote Sens.***2018**, *10*, 643. ; https://doi.org/10.3390/rs10040643

Borbas, E.E., M. Feltz, 2019: Updating the CAMEL surface emissivity atlas for RTTOV, EUMETSAT NWP SAF Visiting Scientist Report, NSPSAF-MO-VS-058, https://www.nwpsaf.eu/publications/vs_reports/nwpsaf-mo-vs-058.pdf

Gambacorta, A, The NOAA Unique CrIS/ATMS Processing System (NUCAPS): Algorithm Theoretical Basis Document, 2013, https://pdfs.semanticscholar.org/8f02/7a6e31d08e299c4b79433ee4302b7a8d62cd.pdf

Han, Y., P. Delst, Q. Liu, F. Weng, B. Yan, and J. Derber, 2005: User's Guide to the JCSDA Community Radiative Transfer Model (Beta Version), http://www.star.nesdis.noaa.gov/smcd/spb/CRTM/crtm- code/CRTM_UserGuide-beta.pdf.

Hayden, C. M., 1988: GOES-VAS simultaneous temperature-moisture retrieval algorithm. *J. Appl. Meteor*., **27**, 705–733.

Hulley, G.; Hook, S. *AG5KMMOH: ASTER Global Emissivity Dataset, Monthly, 0.05 degree, HDF5 V041*; NASA EOSDIS Land Processes DAAC, USGS Earth Resources Observation and Science (EROS) Center: Sioux Falls, SD, USA, 2016.

Li, J., W. Wolf, W. P. Menzel, W. Zhang, H.-L. Huang, and T. H. Achtor, 2000: Global soundings of the atmosphere from ATOVS measurements: The algorithm and validation, *J. Appl. Meteorol.,* 39: 1248–1268.

____, C. C. Schmidt, J. P. Nelson, T. J. Schmit, and W. P. Menzel 2001: Estimation of total ozone from GOES sounder radiances with high temporal resolution. *J. Atmos. Oceanic Technol*., **18,** 157–168.

Saha, S., S. Moorthi, H. Pan, X. Wu, J. Wang, and Coauthors, 2010: The NCEP Climate Forecast System Reanalysis. *Bulletin of the American Meteorological Society*, **91**, 1015–1057, doi:10.1175/2010BAMS3001.1

Salisbury, J.W., and D.M. D'Aria, 1992: Emissivity of terrestrial materials in the 8-14mm atmospheric window. *Remote Sensing of the Environment*, **42**, 83-106.

Seemann, S. W., J. Li, W. P. Menzel, and L. E. Gumley, 2003. Operational retrieval of atmospheric temperature, moisture, and ozone from MODIS infrared radiances. *J. Appl. Meteor*., **42**, 1072 1091.

____, Borbas, E.E., Knuteson, R.O., Stephenson, G.R., and Huang, H-L., 2008: Development of a global infrared emissivity database for application to clear sky sounding retrievals from multi-spectral satellite radiances measurements. *J. Appl. Meteorol. and Clim.* 47, *108–123*

Hook, S. CAM5K30EM: Combined ASTER and MODIS Emissivity for Land (CAMEL) Emissivity Monthly Global 0.05 Deg. V001; NASA EOSDIS Land Processes DAAC, USGS Earth Resources Observation and Science (EROS) Center: Sioux Falls, SD, USA, 2017. DOI: 10.5067/MEaSUREs/LSTE/CAM5K30EM.001

Saunders, R., Hocking, J., Turner, E., Rayer, P., Rundle, D., Brunel, P., Vidot, J., Roquet, P., Matricardi, M., Geer, A., Bormann, N., and Lupu, C., 2018: An update on the RTTOV fast radiative transfer model (currently at version 12), Geosci. Model Dev., 11, 2717-2737, https://doi.org/10.5194/gmd-11-2717-2018.

Smith, W. L., Woolf, H. M., and W. J. Jacob, 1970: A regression method for obtaining real-time temperature and geopotential height profiles from satellite spectrometer measurements and its application to Nimbus 3 "SIRS" observations. *Mon. Wea. Rev..*, **8**, 582–603.

____, and H. M. Woolf, 1988: A Linear Simultaneous Solution for Temperature and Absorbing Constituent Profiles from Radiance Spectra. Technical Proceedings of the Fourth International TOVS Study Conference held in Igls, Austria 16 to 22 March 1988, W. P. Menzel Ed., 330–347.

____, Woolf, H. M., Nieman, S. J., and T. H. Achtor, 1993: ITPP-5 - The use of AVHRR and TIGR in TOVS Data Processing. Technical Proceedings of the Seventh International TOVS Study Conference held in Igls, Austria 10 to 16 February 1993, J. R. Eyre Ed., 443–453.

____, E. Weisz, S. Kireev, D. Zhou Z. Li and E. Borbas, 2012: Dual-Regression Retrieval Algorithm For Real-time Processing of Satellite Ultraspectral Radiances, *J. Appl. Meteor. Climatol.*, **51**, 1455–1476. doi: http://dx.doi.org/10.1175/JAMC-D-11-0173.1

Sun, B., A. Reale, F. H. Tilley, M. E. Pettey, N. R. Nalli and C. D. Barnet, Assessment of NUCAPS S-NPP CrIS/ATMS Sounding Products Using Reference and Conventional Radiosonde Observations, in *IEEE Journal of Selected Topics in Applied Earth Observations and Remote Sensing*, vol. 10, no. 6, pp. 2499-2509, June 2017. doi: 10.1109/JSTARS.2017.2670504

Veglio P., R. Holz, L. Gumley, G. Quinn, S. Dutcher, and B. Flynn, 2018, Yori: L3 Gridding Tools, Version 1.3.7, https://sips.ssec.wisc.edu/docs/yori.html

Ware, R.H. D. W. Fulker, S. A. Stein, D. N. Anderson, S. K. Avery, R. D. Clark, K. Droegemeier, J. P. Kuettner, J. B. Minster, and S. Sorooshian, 2000: SuomiNet: A real-time national GPS network for atmospheric research and education. *Bulletin of the American Meteorological Society* 81, 677–694.

Weisz, E., B. A. Baum, and W. P. Menzel, 2017: Fusion of Satellite-Based Imager and Sounder Data to Construct Supplementary High Spatial Resolution Narrowband IR Radiances. *J. of Applied Remote Sensing*, 11(3), 036022 (2017). https://doi.org/10.1117/1.JRS.11.036022

7.1. Data References

AIRS-only L3 data: AIRS Science Team/Joao Teixeira (2013), AIRS/Aqua L3 Daily Support Product (AIRS-only) 1 degree x 1 degree V006, Greenbelt, MD, USA, Goddard Earth Sciences Data and Information Services Center (GES DISC), Accessed: [Jun 2016], 10.5067/Aqua/AIRS/DATA306

AIRS+AMSU_HSB L3 data: AIRS Science Team/Joao Teixeira (2013), AIRS/Aqua L3 Monthly Support Monthly Product (AIRS+AMSU+HSB) 1 degree x 1 degree V006, Greenbelt, MD, USA, Goddard Earth Sciences Data and Information Services Center (GES DISC), Accessed: [Jun 2016], 10.5067/Aqua/AIRS/DATA323

GPS data: Atmospheric Radiation Measurement (ARM) user facility. 2001, updated hourly. SuomiNet Global Positioning System (30SUOMIGPS). Jan 2012 to July 2015, Southern Great Plains (SGP) External Data (satellites and others) (X1). Compiled by L. Ma, R. Wagener and L. Gregory. ARM Data Center. Data set accessed Jun 2018 at http://dx.doi.org/10.5439/1350679

MWR data: Atmospheric Radiation Measurement (ARM) user facility. 2006, updated hourly. Microwave Radiometer - High Frequency (MWRHF). Jan 2012 to July 2015 , Southern Great Plains (SGP) Central Facility, Lamont, OK (C1). Compiled by M. Cadeddu and V. Ghate. ARM Data Center. Data set accessed Jun 2018 at http://dx.doi.org/10.5439/1025250

MYD07 L2 data: Borbas, E., et al., 2015. MODIS Atmosphere L2 Atmosphere Profile Product. NASA MODIS Adaptive Processing System, Goddard Space Flight Center, USA: http://dx.doi.org/10.5067/MODIS/MYD07_L2.006

MYD08 L3 data: Platnick, S., et al., 2017. MODIS Atmosphere L3 Monthly Product. NASA MODIS Adaptive Processing System, Goddard Space Flight Center, USA: http://dx.doi.org/10.5067/MODIS/MOD08_M3.061

SSMI TPW data: Remote Sensing Systems, 2016. Monthly Mean Total Precipitable Water Data Set on a 1 degree grid made from Remote Sensing Systems Version-7 Microwave Radiometer Data, V07r01, [accessed on Jun 2016]. Santa Rosa, CA, USA. Available at: www.remss.com

WATVP_L2_VIIRS_SNPP data: Borbas, E.E., et al., 2019, VIIRS/SNPP Level-2 Daily Mean Water Vapor Products. NASA MODIS Adaptive Processing System, Goddard Space Flight Center, USA: https://dx.doi.org/10.5067/VIIRS/WATVP_L2_VIIRS_SNPP.001
10.5067/VIIRS/WATVP_L2_VIIRS_SNPP.001

WATVP_D3_VIIRS_SNPP data: Borbas, E.E., et al., 2019, VIIRS/SNPP Level-3 Daily Mean Water Vapor Products. NASA MODIS Adaptive Processing System, Goddard Space Flight Center, USA: https://dx.doi.org/10.5067/VIIRS/WATVP_D3_VIIRS_SNPP.001
10.5067/VIIRS/WATVP_D3_VIIRS_SNPP.001

WATVP_M3_VIIRS_SNPP data: Borbas, E.E., et al., 2019, VIIRS/SNPP Level-3 Monthly Mean Water Vapor Products. NASA MODIS Adaptive Processing System, Goddard Space Flight Center, USA: https://dx.doi.org/10.5067/VIIRS/WATVP_M3_VIIRS_SNPP.001
10.5067/VIIRS/WATVP_M3_VIIRS_SNPP.001